Chemistry & Biology, Vol. 11, 99–106, January, 2004, ©2004 Elsevier Science Ltd. All rights reserved. DOI 10.1016/j.chembiol.2003.12.017

Design, Synthesis, and Characterization of Urokinase Plasminogen-Activator-Sensitive Near-Infrared Reporter

Benedict Law,[1] Alejandro Curino,[2] Thomas H. Bugge,[2] Ralph Weissleder,[1] and Ching-Hsuan Tung[1,*]
[1]Center for Molecular Imaging Research
Massachusetts General Hospital
Harvard Medical School
Charlestown, Massachusetts 02129
[2]Proteases and Tissue Remodeling Unit
Oral and Pharyngeal Cancer Branch
NIDCR
National Institute of Health
Bethesda, Maryland 20892

Summary

The urokinase-type plasminogen activator (uPA) plays a critical role in malignancies, and its overexpression has been linked to poor clinical prognosis in breast cancer. The ability to noninvasively and serially map uPA expression as a biomarker would thus have significant potential in improving novel cancer therapies. Here, we describe the development of a selective uPA activatable near-infrared (NIR) fluorescent imaging probe. The probe consists of multiple peptide motifs, GGSGRSANAKC-NH_2, terminally capped with different NIR fluorochromes (Cy5.5 or Cy7) and a pegylated poly-*L*-lysine graft copolymer. Upon addition of recombinant human uPA to the probe, significant fluorescence amplification was observed, up to 680% with the optimized preparation. No activation with negative control compounds and uPA inhibitors could be measured. These data indicate that the optimized preparation should be useful for imaging uPA in cancer.

Introduction

The urokinase plasminogen activator (uPA) and the uPA receptor (uPAR) have been shown to facilitate cancer cell invasion into surrounding tissue [1–3] by breaking down basement membranes and interstitial matrix [4, 5]. Urokinase plasminogen activator is an exogenous 52 kDa serine protease with multiple enzymatic activities [6] that depend on binding to its cell surface receptor uPAR [7]. For example, uPA binding to uPAR converts inactive plasminogen into active plasmin, which in turn degrades many extracellular proteins including lamin, fibronectin, and fibrin [7]. uPA is also known to directly activate certain matrix metalloproteinases [8], vascular endothelial growth factor (VEGF), and human growth factor (HGF) [9]. uPA/uPAR binding is also involved in gene transcription [7].

High levels of uPA and uPAR have been found in many different types of malignancies [10]. In some studies of breast [10, 11] and bladder cancer [12], the expression levels of uPA have been correlated with the prognosis. The ability to noninvasively map uPA expression repeatedly would thus be an important adjunct to current diagnostic approaches. Enzyme-linked immunosorbent assays (ELISAs) [12–14] and immunohistochemistry [15] are commonly used methods to detect uPA expression in tissue specimens. Although these techniques are currently used as the golden standards for analysis of biopsy and surgical specimens, the procedures do not allow for the direct monitoring of the entire tumors in vivo serially over time.

Here, we report on the synthesis, characterization, and optimization of uPA sensing near-infrared fluorescence (NIRF) imaging agents. The approach is based on substrate-mediated cleavage of NIRF probe from structurally constrained (and thus quenched) biocompatible precursors. Using multiple uPA substrate motifs (GGSGRSANAKC-NH_2) attached to a pegylated graft copolymer [16], we show highly sensitive uPA cleavage, fluorescence amplification, and the ability to image uPA inhibition.

Results and Discussion

Design of the uPA-Selective Probes

The designed uPA probes consisting of three components (Figure 1): (1) a nonimmunogenic copolymer of *L*-lysine (PLL) and methoxy poly(ethylene glycol) (MPEG) as a backbone for substrate attachment and improved tumoral delivery [16], (2) peptide substrates specifically recognized and cleaved by uPA, and (3) the terminal conjugated near-infrared (NIR) fluorochromes as reporters [17]. Use of NIRF, rather than visible fluorochromes, enables more efficient photon collection in biological tissues, due to better tissue penetration, lower scattering, and lower autofluorescence in the near-infrared range [18]. Cy5.5 (Ex/Em = 675/694 nm) and Cy7 (Ex/Em = 747/776 nm) were initially selected as model fluorophores given their distinct excitation and emission wavelengths. The imaging probes were designed so that the fluorochromes were assembled in close proximity, resulting in efficient fluorescence quenching (Figure 1). Upon uPA-selective enzymatic cleavage, the fluorochromes are released from the delivery backbone, resulting in fluorescence signal.

Evaluation of the uPA Substrate Specificity and Its Cleavage Site

The peptide sequence LGGSGRSANAILE-NH_2 has been reported [19] as a highly potent substrate for uPA. It contains the primary motif SGRSA, which is cleaved 840 times (k_{cat}/K_m = 1200 $M^{-1}s^{-1}$) more efficiently than the native sequence (KKSPGRVVGGSVAH) from plasminogen. Here, we modified the parent sequence to GGSGRSANAKC-NH_2 so that an internal fluorescent marker, fluorescein isothiocyanate (Fitc), could be attached to the amino side chain of the lysine residue during solid-phase peptide synthesis. The introduction of Fitc was used to easily quantify and follow peptide

*Correspondence: tung@helix.mgh.harvard.edu

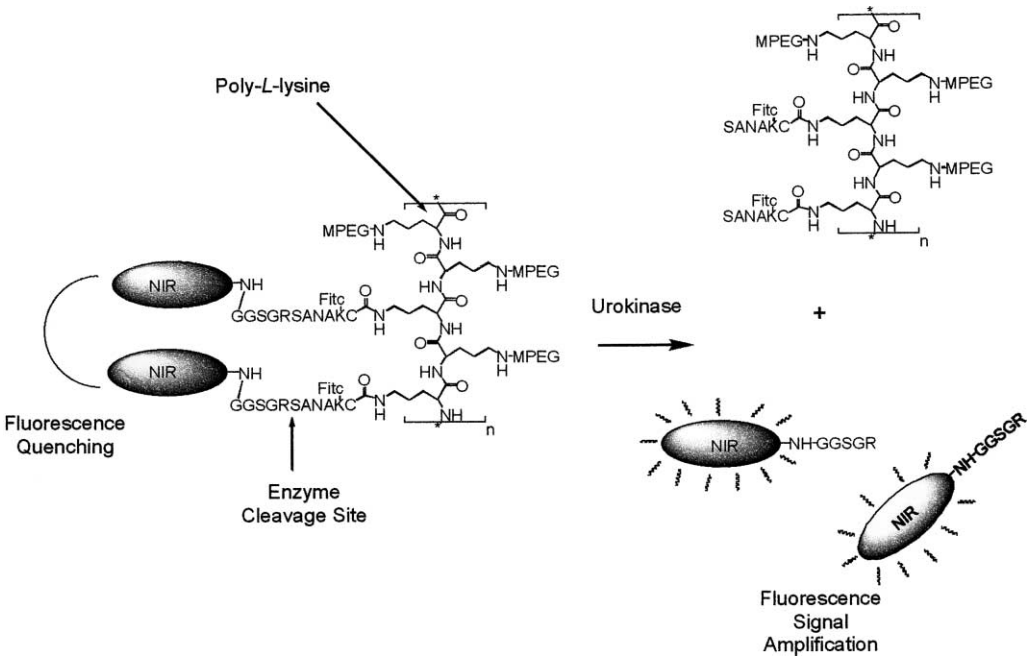

Figure 1. Schematic Representation of Protease Selective Probe

The probe is composed with a poly-*L*-lysine backbone. The peptide substrate was conjugated to a synthetic graft copolymer to promote efficient tumoral delivery. The close spatial proximity of the multiple substrates leads to fluorescence quenching in the bound state. Upon enzymatic cleavage, the released peptide fragments result in fluorescence signal amplification.

substrates during subsequent conjugation and purification steps. The C-terminal cysteine residue was introduced to provide a thiol-reactive site for peptide conjugation to the iodoacetylated PLL-MPEG copolymer. A scrambled sequence, GGSGASNRAK(Fitc)C-NH_2, was also synthesized as a control in which the residues between P1 and P3′ were rearranged. Prior to the attachment of the uPA substrates to the graft copolymer, we confirmed their specificity for uPA by HPLC. Initial studies indicated that the uPA substrate peptide, GGS GRSANAK(Fitc)C-NH_2, formed an intermolecular dimer via a disulfide linkage in aqueous buffer (data not shown). We therefore modified the original sequence to GGSGRSANAK(Fitc)A-NH_2 for enzymatic studies by replacing the C-terminal cysteine residue with an alanine residue. HPLC chromatography (Figure 2A) indicated that this substrate sequence was indeed recognized and specifically cleaved by uPA. MALDI-TOF MS analyses (Figure 2B) showed that the digested compound appeared as a single peak at 949.98 Da, which corresponds to the mass ions $[M + H]^+$ of SANAK(Fitc)A-NH_2. The site of cleavage was located between the serine and arginine residue (GGSGR↓SANAK(Fitc)A-NH_2), in accordance with what has been previously reported [19]. There was no enzymatic cleavage of the scrambled control peptide, GGSGASNRAK(Fitc)A-NH_2. Likewise, cleavage of the substrate peptide was abrogated in the presence of excess uPA inhibitor, amiloride (Figure 2A) [20].

Synthesis and Characterization of the uPA-Selective Probes

The synthetic method for the attachment of protease-specific substrates to the PLL-MPEG graft-copolymer was modified from a previously reported procedure [21] (Figure 3A). Iodoacetic anhydride was first coupled to the free amino groups of PLL-MPEG. This allows for the subsequent peptide attachment via a thiol-specific reaction and additionally blocks any reactive amino group on the PLL backbone. Dimethyl formamide (DMF) was used as solvent for peptide conjugation to iodoacetylated PLL-MPEG copolymer. This optimized method also resulted in consistent peptide loading of 17–19 peptides per PLL-MPEG copolymer. Commercially available Cy5.5 and Cy7 monofunctional hydroxysuccinamides were finally attached to the N-terminal glycines of peptide substrates. Reactions were monitored and characterized by UV absorbance. Both the Cy5.5 and Cy7 uPA-selective probes showed an absorbance λ_{max} at 494 nm, indicating the presence of the peptide marker Fitc (Figure 3B). Additional absorbance peaks for Cy5.5 and Cy7 were observed at 675 nm and 757 nm, respectively. All probes had a high loading efficiency of 88%– 98%, resulting in an average of 15–19 fluorophores per assembled imaging agent (Table 1). The imaging probes were stable in aqueous buffer at 4°C for at least 3 months.

Activation of the Imaging Probes

Activation of fully assembled imaging probes was tested by fluorescence spectrophotometry. Incubation of the Cy5.5 uPA-selective probe with uPA resulted in a 680% change in fluorescence over time and reached plateau within 2 hr (Figure 4A). In contrast, the control probe with uPA showed essentially no changes in fluorescence. As expected, no fluorescence signal changes were observed without the addition of uPA. To confirm whether NIRF activation was protease dependent, different con-

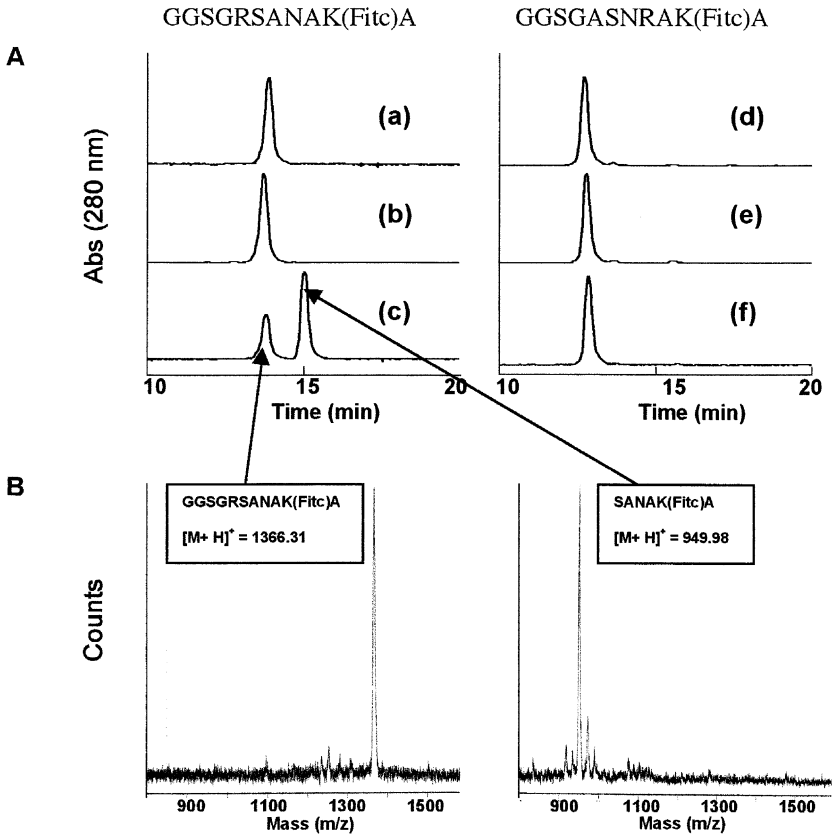

Figure 2. Specificity of Peptide Substrates

(A) HPLC chromatogram of (a–c) uPA substrate, GGSGRSANAK(Fitc)A, and (d–f) scrambled control, GGSGASNRAK(Fitc)A: (a) substrate alone; (b) substrate in the presence of urokinase and inhibitor (amiloride); (c) substrate in the presence of urokinase; (d) control alone; (e) control in the presence of urokinase and inhibitor (amiloride); and (f) control in the presence of urokinase.

(B) The MALDI-TOF mass spectra of urokinase substrate (left) and its digested product (right).

centrations (0, 1, 1.7, 2.0, 2.7, and 3.0 μM) of amiloride [14], a uPA inhibitor, were applied to block the enzymatic activity prior to the addition of Cy5.5 uPA-selective probes. The fluorescence emissions of each sample were recorded at a fixed time point of 2 hr (Figure 4B). A linear plot ($r^2 > 0.989$) of fluorescence changes of Cy5.5 uPA selective probe versus Log [amiloride] indicated that half reduction of NIRF activation was achieved with 63 μM of inhibitor (Figure 4B, inset).

Comparison of Cy5.5 and Cy7 as Reporter Fluorochromes

In the following experiments, we wished to determine whether the peptide terminal fluorochrome would have an effect on the magnitude of fluorescence activation. Surprisingly, the uPA-selective probe that labeled with Cy7 showed a lower increase in fluorescence (moderate 2.2-fold increase) compared to the Cy5.5 probe (5.8-fold increase) under identical experimental conditions (Figure 4C). It is possible to explain the results by different self-quenching properties of the fluorochromes; however, recent studies have shown that antibodies labeled with either Cy5.5 and Cy7 succinimidyl esters have similar quenching efficiencies [22]. In order to further understand our observations, we calculated the fluorescence recovery by dividing the fluorescence intensities of the enzyme-cleaved probes at a particular fluorochrome concentration with the fluorescence intensities of the corresponding concentrations of free fluorophore (Figure 4D). With 91% of Cy5.5 loading, 98% of the fluorescence could be recovered. In contrast, with 98% of Cy7 loading, only 8% of fluorescence could be recovered. It was also found that Cy7 fluorescence recovery (%) decreased inversely with fluorophore loading. However, the recovery was not complete even with 25% of Cy7 loading. It has been reported that certain cyanine fluorophores self-aggregate in solution [22], and this effect depends on their structure, pH, ionic strength, concentration, solvent polarity, electrolyte, and temperature [23]. When comparing the chemical structures of Cy5.5 and Cy7 (Figure 3A), the latter has fewer sulfonate groups and an extra methine group that contributes to hydrophobicity, which may be responsible for aggregate formation or for intramolecular hydrophobic interaction and result in steric hindrance from the enzyme reactive site for probe activation.

In Vitro Imaging of Probes

Both the Cy5.5 and Cy7 uPA-selective probes were subsequently tested using a NIRF reflectance imaging sys-

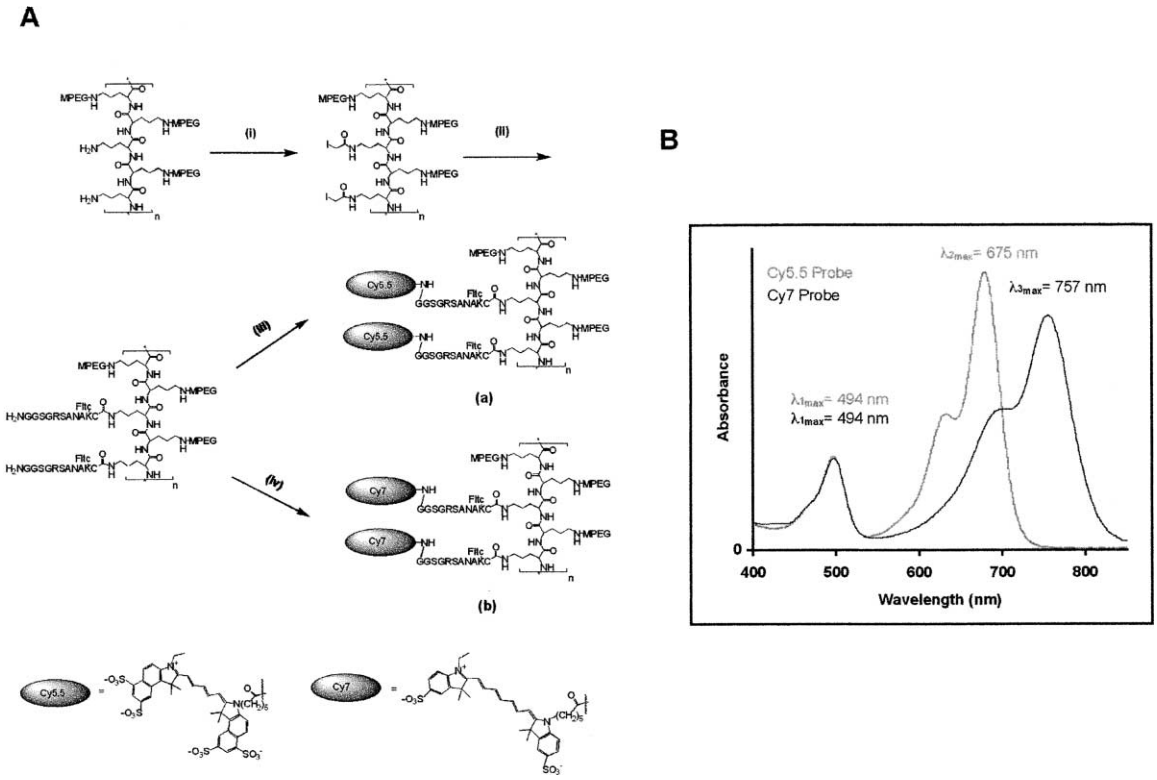

Figure 3. Synthesis and Characterization of uPA-Selective Probes

(A) Synthetic scheme of urokinase-selective probes with (a) Cy5.5 and (b) Cy7 attached as the fluorophores. (I) Iodoacetic anhydride/DIPEA/DMF/room temperature/3 hr; (II), peptide substrate GGSGRSANAK(Fitc)C/DMF/room temperature/8 hr; (III), Cy5.5 mono NHS ester/$NaHCO_3$/room temperature/3 hr; and (IV), Cy7 mono NHS ester/$NaHCO_3$/room temperature/3 hr.

(B) UV absorbance spectrum of the Cy5.5- and Cy7-labeled uPA-selective probes (where λ_{1max} = Fitc, λ_{2max} = Cy5.5, and λ_{3max} = Cy7).

tem [24]. To compensate for the differences in activation, the exposure time and the number of images collected for analysis were adjusted accordingly (Figure 5A). Band-pass filters were employed to adjust the excitation wavelength for Cy 5.5 (615–645 nm) and Cy7 (716–756 nm), respectively, while the corresponding emission band-pass filters were used to collect the emission signal from 680 to 720 nm for Cy5.5 and 780 to 820 nm for Cy7. A 6-fold increase in fluorescence signal was detected with the Cy5.5 uPA-selective probe within 2 hr after uPA addition (Figure 5B). In contrast, only trace amounts of fluorescence were observed in the control probes that containing the scrambled peptide sequence. These unwanted signals were attributed to the dye molecules that are conjugated onto the polymer system. Images observed in the Cy7 channel showed a 2.9-fold increase in fluorescence activation from the Cy7 uPA-selective probe (Figure 5C). Note that there are no fluorescence emissions from any of the probes when they are not excited from their corresponding channels; this should ultimately allow the detection of multiple enzymes.

Table 1. Coupling Efficiency of NIR Fluorochromes to the Peptide Synthetic Graft Copolymer

Probe Components		Fluorochromes/Probe	Coupling Efficiency (%)
Substrate	Cy5.5	17	91
	Cy7	19	98
Control	Cy5.5	16	97
	Cy7	15	88

Coupling efficiency was calculated by dividing the fluorophore concentration by the concentration of peptide marker (Fitc).

Detection of uPA Activity in Biological Samples

We further investigated the application of uPA-selective probe for detection of urokinase in biological samples. The biological role of uPA has been extensively studied by using uPA-deficient mice (C57BL6/J-uPA$^{-/-}$) [25–27]. Typically, the activity of plasminogen was examined by casein-plasminogen zymography [28]. With the specific information obtained from the above experiments, we reasoned that the developed uPA probe could be applied to determine uPA activity in zymography. To investigate this possibility, urine samples from wild-type C57BL6/J mice and uPA knockout C57BL6/J-uPA$^{-/-}$ mice were collected, and the uPA expression was analyzed by traditional casein-plasminogen zymography. As expected, uPA ($\sim$48 kDa) was only found in the wild-type (C57BL6/J) urine but not in the C57BL6/J-uPA$^{-/-}$ sample (Figures 6A and 6B). The higher band at $\sim$70 kDa indicated the expression of tissue plasminogen (tPA). We then cast the SDS-PAGE (7.5% v/v) gel with

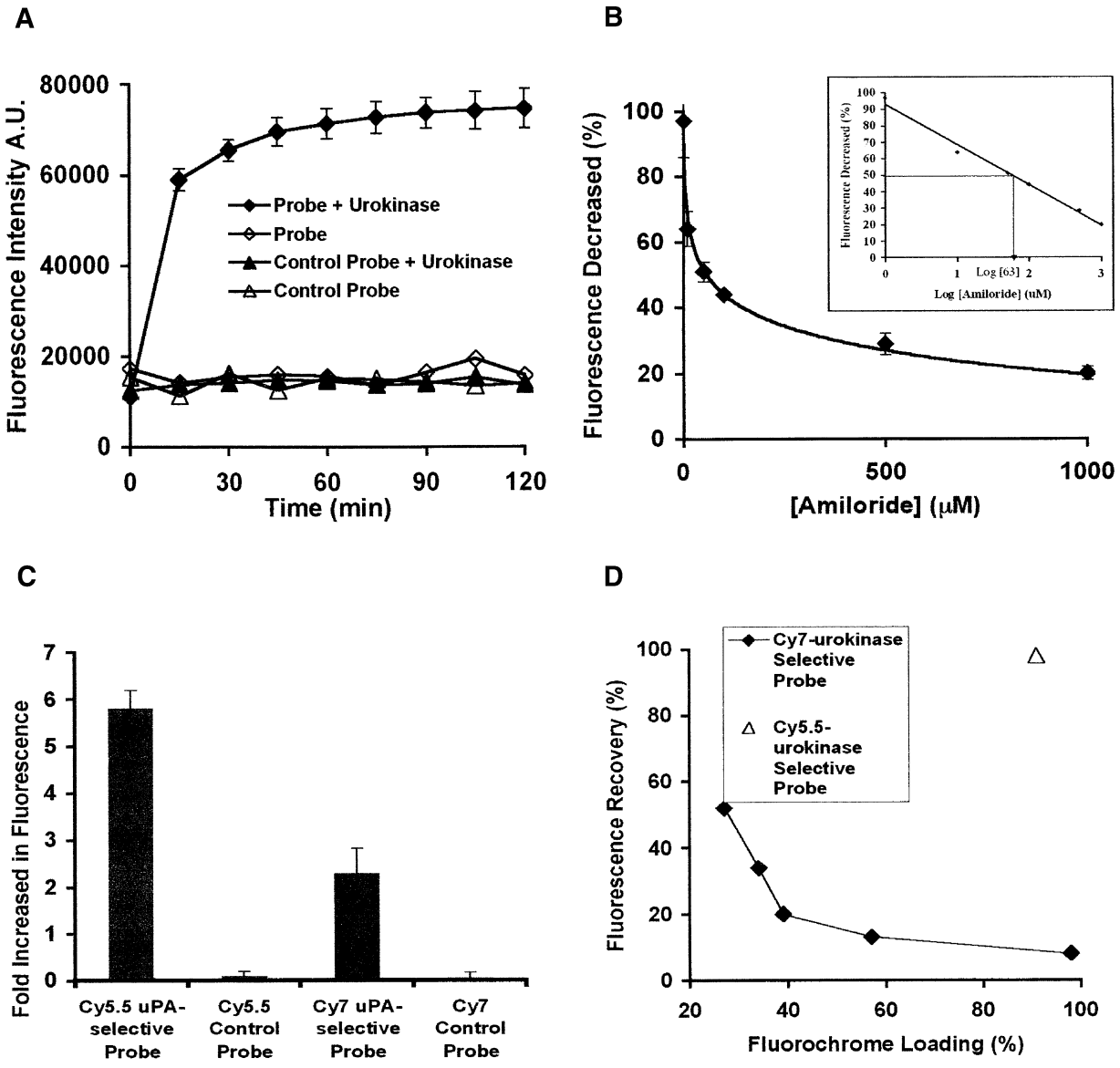

Figure 4. In Vitro Activation and Inhibition of uPA-Selective Probes

(A) Fluorescence intensity versus time scale (min) on activation of the Cy5.5-labeled probes (200 nM) with urokinase.

(B) Fluorescence changes of Cy5.5 uPA-selective probe (200 nM) versus amiloride concentration (μM) at 2 hr after the addition of urokinase. Inset: fluorescence emission reduces by 50% in the presence of 63 μM amiloride.

(C) Comparison of fold increase in fluorescence of Cy5.5 and Cy7 uPA-selective probes on activation with urokinase 2 hr after addition.

(D) Percentage of fluorophore loadings on the uPA-selective probe versus percentage of fluorescence recovery ([Fluorescence Intensity$_{\text{fluorophore-selective probe}}$/Fluorescence Intensity$_{\text{free fluorophore}}$] × 100%).

Cy5.5 uPA-selective probe for optical zymography. Urine samples were prepared as previously described for regular casein-plasminogen zymography. After electrophoresis, the separated proteins were renatured by incubations in 2.5% (v/v) Triton X-100 solution. Under the Cy5.5 channel, a bright band corresponding to uPA (~48 kDa) in C57BL6/J urine was found coeluted with human recombinant urokinase in the gel (Figure 6C). No uPA activity was found in the sample collected from the knockout animal. Notably, the tPA band (~70 kDa) observed in the regular casein-plasminogen zymography was not found in this optical zymographic gel. The results indicate that the developed probe is very selective for uPA. Other proteins and enzymes in the urine sample cannot activate the probe, resulting in no fluorescence signal changes.

Significance

Degradation of the extracellular matrix is a prerequisite for invasive growth and metastatic spread of tumors. Several reports have indicated that uPA is a possible predictor of disease outcome [10]. The above studies demonstrate that it is feasible to design and

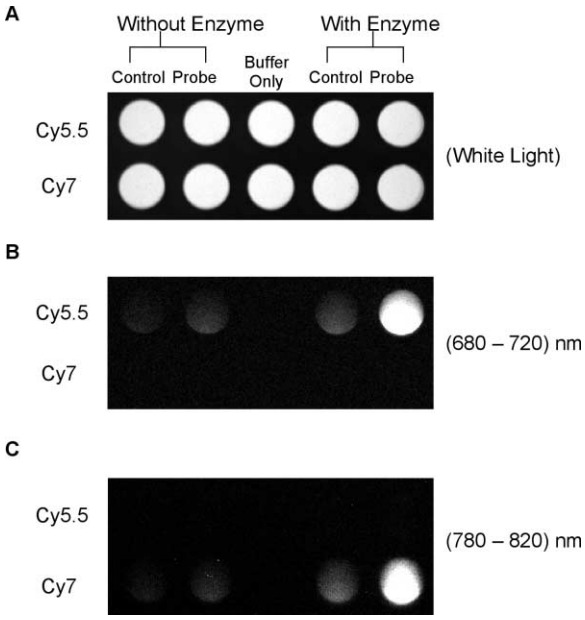

Figure 5. In Vitro Activation of uPA and Control Probes

Images of Cy5.5 and Cy7 uPA-selective probes and their scrambled control probes (200 nM) when monitored in (A) white light, (B) 680–720 nm (Cy5.5) and (C) 780–820 nm (Cy7) emission channels at 2 hr after the addition of urokinase (1.89 units) in Tris-HCl buffer (50 mM) containing NaCl (50 mM, pH 7.4).

synthesize uPA-specific NIRF imaging probes. Specifically, we show over 6-fold increases in NIRF signal upon uPA activation with the optimized probes. So far, the Cy5.5 containing reporter probe seems superior in terms of activation ratios and should represent an ideal probe for subsequent NIRF testing. Similarly, as shown for other proteases (e.g., cathepsin B [29], cathepsin D [21], and MMPs [30]), this would involve testing in tumor models by reflectance [24] or tomographic [18] imaging methods. Based on the superior quenching properties of the uPA probe, we have developed an optical zymography analysis. The method is specific to uPA activity and is sensitive enough to detect a small amount of enzyme in biological samples. Overall, we believe that the developed uPA imaging probe should be a valuable adjunct to existing probes, as uPA is critically involved in many cellular and tissue processes, including tumor invasion, metastasis formation, angiogenesis, and tissue remodeling. Given its broad role, uPA has also been proposed as a therapeutic target [20, 31], and the developed imaging probes could be used as a direct biomarker to assess therapeutic efficacy.

Experimental Procedures

Chemicals

All solvents were purchased from Fisher Scientific (Fair Lawn, NJ). All reagents for peptide synthesis were supplied by Novabiochem (San Diego, CA). Cy5.5 and Cy7 monofunctional hydroxysuccinamide ester were purchased from Amersham Pharmacia (Piscataway, NJ). Amiloride, anisole, ethandithiol, fluorescein isothiocyante, thioanisole, urokinase, and all other chemical reagents were purchased from Sigma-Aldrich (St. Louis, MO).

Peptide Synthesis

Peptide synthesis was performed on an automated solid-phase peptide synthesizer (PS3, Rainin, Woburn, MA) employing the traditional N_α-Fmoc methodology on Rink Amide resin (162 mg, 0.1 mmol). Side-chain protections were Arg(Pbf), Asn(Trt), Cys(Trt), Lys(ivDde), and Ser(tBu). All amino acids (4 eq.) were attached to the resin by stepwise elongation using 2(1H-benzotriazole-1-yl)-1,1,3,3-tetramethyluronium hexafluorophosphate (HBTU)/*N*-hydroxybenzotriazole (HOBt)/*N*-methyl morpholine (4/4/8 eq.) as the coupling reagents in DMF (10 ml). The peptide N terminus was blocked by introduction of N-α-*t*-Boc-glycine. The resulting peptide resin was washed three times with 2% (v/v) hydrazine monohydrate in DMF (5 ml) for 3 min to selectively remove ivDde (4,4-dimethyl-2,6-dioxocyclohexylidene)3-methylbutyl) side-chain amino protecting group. Fitc (151 mg, 0.4 mmol) dissolved in DMSO (4 ml) was then added to the resin. The reaction was initiated with the addition of *N,N*-diisopropylethylamine (DIPEA) (1 ml) and was subjected to further gentle shaking for 8 hr at room temperature. Cleavage of the peptides from the resin and side-chain deprotection employed a mixture of TFA/thioanisole/ethanedithiol/anisole: 90/5/3/2 (5 ml) for 3 hr at room temperature, which was then precipitated into methyl-*tert*-butyl ether at 4°C. Crude peptides were purified by HPLC (Ranin, Worburn, MA) to >95% homogeneity. MALDI-TOF mass spectrometry (Tufts Protein Chemistry Facility, Medford, MA) confirmed the expected mass ions for all synthetic peptides. All peptide concentrations were determined by UV absorbance for its attached Fitc moiety ($\epsilon = 75 \times 10^{-3}$ $M^{-1}cm^{-1}$ at 494 nm) at pH 9.

Specificity of Peptide Substrate

The peptide substrate GGSGRSANAK(Fitc)A (0.27 μg, 0.2 nmol) and the scrambled control peptide GGSGASNRAK(Fitc)A (0.27 μg, 0.2 nmol) were incubated with human urokinase (urine, 100 μl, 18.9 unit) in Tris-HCl buffer (200 μl, 50 mM, pH 7.4) containing NaCl (100 mM) for 3 min. Amiloride (20 μl, 2.5 mM) was used as an inhibitor for urokinase. The enzyme was then removed by centrifugal filtration (Microcon YM-50), and the filtrate (20 μl) was collected and monitored by HPLC (Vydac 218TP54 Reversed Phase C-18 Column, 4.6 × 250 mm). The solution mixture was eluted using a linear gradient starting at 0 min with 18% of 90% (v/v) acetonitrile in 0.1% (v/v) TFA in deionized water and ending at 30 min with 30% of 90% (v/v)

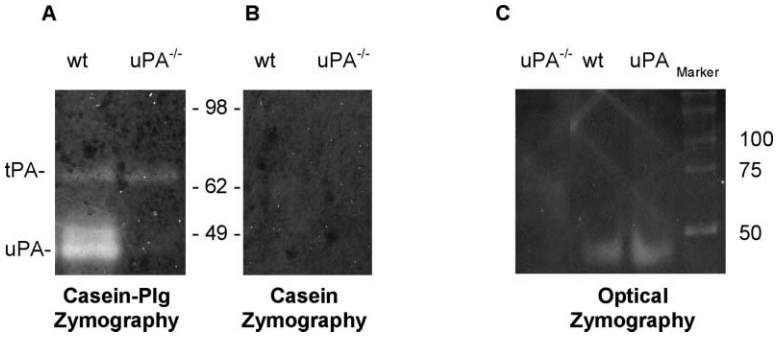

Figure 6. The Application of uPA-Selective Probe for Optical Zymography

(A and B) Plasminogen-casein (A) and casein (B) zymographies confirmed the presence of uPA in urine from a wild-type (wt) mouse (C57BL6/J) and indicated that the enzyme is absent in gene knockout mouse (C57BL6/J-uPA$^{-/-}$).

(C) NIR image of optical zymography. Note that only the uPA band was found in the wild-type sample. Other enzymes, including tPA, in the urine sample could not recognize the probe and therefore generated no fluorescence signal.

acetonitrile in 0.1% (v/v) TFA in deionized water. The flow rate was set at 1 ml/min. Peak elution was monitored at 280 nm, and the absorbance was recorded from 10 to 20 min. The eluted fractions were separated and collected for further analysis of digested products by MALDI-TOF mass spectrometry.

Synthesis of uPA-Selective Imaging Probes

Protected graft copolymer with a poly-*L*-lysine backboned (PLL) and methyoxy poly(ethylene glycol) (MPEG) side chains was prepared as previously described [16]. The uPA probe synthesis was modified from previously developed protocol [21]. Briefly, PLL-MPEG (4 mg, 8.8 nmol) was dissolved in DMF (100 μl) and was added to iodoacetic anhydride (8 mg, 22.84 μmol) in DMF (100 μl) with DIPEA (20 μl) for 3 hr at 37°C. The reaction mixture was then washed with 50% (v/v) DMF in water and purified by centrifuging through a 50 kDa cutoff filter (Microcon YM-50) to remove any excess reagents, byproducts, and solvents. No free amino groups were found on the iodoacetylated PLL-MPEG, as monitored by a TNBS assay. The compound was then redissolved in DMF (200 μl) and coupled with the peptide substrate GGSGRSANAK(Fitc)C (8 mg, 5.74 μmol) or the scrambled control peptide GGSGASNRAK(Fitc)C (8 mg, 5.74 μmol) through a thiol-specific reaction for 6 hr at room temperature. The reaction mixture was then diluted with water to 500 μl and loaded onto a size-exclusion column (P-10 bio-gel, Bio-Rad, Hercules, CA) to remove any excess peptides or byproducts. Coupling efficiency was determined based on the extinction coefficient of the peptide marker (Fitc moiety), indicating there was an average of 18–20 peptides coupled to each PLL-MPEG molecule. To introduce near-infrared fluorophores to the copolymers, Cy5.5 monofunctional hydroxysuccinamide (0.2 mg, 177 nmol) or Cy7 monofunctional hydroxysuccinamide (0.2 mg, 191 nmol) dissolved in $NaHCO_3$ (50 μl, 0.1 mM) was added to the peptide-PLL-MPEG conjugate (0.1 mg) for 3 hr at room temperature. The reaction mixtures were then washed and purified three times with deionized water (200 μl) with a 50 kDa cutoff filtration device (Microcon YM-50). The residues were then collected and redissolved in water for characterization.

Characterization of Imaging Probes

To determine the number of attached fluorophores to each peptide-PLL-MPEG conjugate, UV absorbance spectra were recorded between 400–850 nm intervals. Both the concentration of peptide marker (Fitc) and fluorophores were determined based on their molar extinction coefficients ($\epsilon_{494} = 75 \times 10^{-3}$ $M^{-1}cm^{-1}$ for Fitc, $\epsilon_{675} = 250 \times 10^{-3}$ $M^{-1}cm^{-1}$ for Cy5.5, and $\epsilon_{747} = 200 \times 10^{-3}$ $M^{-1}cm^{-1}$ for Cy7, according to the manufacturer data sheets) at pH 9.0. Coupling efficiency was then calculated by the molar ratio of the attached fluorophores to the peptide marker. Probes with different coupling efficiencies were also synthesized by altering the reaction time for attachment of activated NIR fluorophores to the peptide-PLL-MPEG conjugate.

Enzymatic Activation

For ease of comparison, all samples of labeled probes were diluted to the same NIRF concentrations (200 nM based on Cy fluorochrome absorption). Activation of the probes with urokinase (20 μl, 1.89 unit) was assayed by fluorescence spectrophotometry (Fluorolog-3, Jobin Yvon, Edison, NJ). The samples, in Tris-HCl buffer (1 ml, 50 mM, pH 7.4) containing NaCl (100 mM), were measured in a 4 mm × 10 mm × 1.5 ml disposable semimicro cuvet. The sample was excited at 674 nm (Cy5.5) and 747 nm (Cy7), and the emission was monitored at 689 nm and 776 nm, respectively. Excitation slit width was set at 5 nm, while the emission slit width was 10 nm. All measurements were performed at 20°C.

Experimental In Vitro Imaging

In vitro imaging was performed using the NIRF reflectance imaging system, which has previously been described [24]. Briefly, the system contains an excitation photon source that emits a broadband white light from a 150 W halogen bulb. Band-pass filters (Omega Optical, Brattleboro, VT) are employed to adjust the corresponding excitation wave bands for Cy 5.5 (615–645 nm) and Cy7 (716–756 nm). Probes and controls (200 pmol of fluorophore contents) in Tris-HCl buffer (200 μl, 50 mM, pH 7.4) containing NaCl (100 mM) were loaded onto individual wells of a clear-bottom 96-well plate (Corning, Corning, NY). Urokinase (20 μl, 1.89 unit) was then added to the appropriate wells, and the plate was incubated for 2 hr at room temperature. It was then exposed to the excitation light source. The corresponding band-pass filters (Omega Optical, Brattleboro, VT) were used to filter the fluorescence emission for 680–720 nm (Cy5.5) and 780–820 nm (Cy7). A 12-bit monochrome CCD camera (Kodak, Rochester, NY) equipped with a 12.5–75 mm zoom lens was used to detect the fluorescent images. The exposure time was 10 s per image for six images in the Cy5.5 channel and 1 min per image for 20 images in the Cy7 channel. The images were further analyzed using computer software (Kodak Digital Science 1D software, Rochester, NY).

Plasminogen-Casein Zymography

Freshly voided urine was collected from a young adult male C57BL6/J-uPA$^{-/-}$ mouse [25, 26] and a matched C57BL6/J mouse (wild-type). The samples were immediately snap frozen in liquid nitrogen. Plasminogen-casein zymography was performed essentially as described [28]. Briefly, aliquots of voided urine (2 μl) were mixed with 2% (w/v) sodium dodecyl sulfate (SDS) sample buffer (2 ml) without reducing agents and separated on 11% (v/v) SDS-PAGE gels that were cast with either 22 mg/ml Glu-Plg (Calbiochem, La Jolla, CA) and 0.64% (w/v) boiled nonfat dry milk powder or with 0.64% (w/v) boiled nonfat dry milk powder alone. The separated proteins were renatured by two 30 min incubations in 2.5% (v/v) Triton X-100, and the gels were incubated overnight at 37°C in glycine (100 mM, pH 8.0). The gels were then stained for 2 hr with 0.1% amido black, destained with 30% (v/v) methanol, 10% (v/v) acetic acid, dried, and scanned.

Optical Zymography

The SDS-PAGE gel (7.5%) was freshly prepared by combining deionized water (4.85 ml), Tris buffer (1.5 M, pH 8.8, 2.5 ml), 10% (w/v) of SDS (100 μl), 30% (w/v) acrylamide containing 1.5% (w/v) bis-acrylamide (2.5 ml), 10% (w/v) ammonium persulfate (50 μl) and TEMED (5 μl). The solution mixture was allowed to shake gently for 2 min. Cy5.5 uPA-selective probe (60 μM of dye content, 30 μl) was then added. The resulting separating gel was poured into a slab gel apparatus (Miniprotean II System, Bio-Rad, 5 cm × 8.5 cm × 1 mm) to a height of 5.5 cm to allow shrinkage to a final height of 5 cm upon polymerization. The acrylamide stacking gel (5%) was composed of deionized water (680 μl), 30% (w/v) acrylamide containing 1.5% (w/v) bis-acrylamide (170 μl), Tris buffer (1.5 M, pH 8.8, 130 μl), 10% (w/v) of SDS (10 μl), 10% (w/v) ammonium persulfate (10 μl), and TEMED (1 μl).

Urine samples (2 μl) from C57BL6/J-uPA$^{-/-}$ or C57BL6/J mice were mixed with 2% (w/v) of SDS (0.5 μl). The diluted samples were then loaded onto the gels without boiling. Human recombinant urokinase (4 ng) was used as the positive control. The separated proteins were renatured by incubations in 2.5% (v/v) Triton X-100 in Tris buffer (50 mM, pH 7.4) for 1 hr. The gel was further washed two times with buffer and imaged by using NIRF reflectance imaging system as described above.

Acknowledgments

The authors would like to thank Dr. Vivien Redeye for the technique assistance. This research was supported by NIH P50-CA86355, NO1-CO17016, RO1 CA99385, and DOD DAMD17-02-1-0693.

Received: June 12, 2003
Revised: October 30, 2003
Accepted: November 3, 2003
Published: January 23, 2004

References

1. Edwards, D.R., and Murphy, G. (1998). Cancer. Proteases–invasion and more. Nature *394*, 527–528.
2. Johnsen, M., Lund, L.R., Romer, J., Almholt, K., and Dano, K. (1998). Cancer invasion and tissue remodeling: common themes

in proteolytic matrix degradation. Curr. Opin. Cell Biol. *10*, 667–671.
3. Koblinski, J.E., Ahram, M., and Sloane, B.F. (2000). Unraveling the role of proteases in cancer. Clin. Chim. Acta *291*, 113–135.
4. Liotta, L.A., Steeg, P.S., and Stetler-Stevenson, W.G. (1991). Cancer metastasis and angiogenesis: an imbalance of positive and negative regulation. Cell *64*, 327–336.
5. Mignatti, P., and Rifkin, D.B. (1993). Biology and biochemistry of proteinases in tumor invasion. Physiol. Rev. *73*, 161–195.
6. Reuning, U., Magdolen, V., Wilhelm, O., Fischer, K., Lutz, V., Graeff, H., and Schmitt, M. (1998). Multifunctional potential of the plasminogen activation system in tumor invasion and metastasis. Int. J. Oncol. *13*, 893–906.
7. Andreasen, P.A., Kjoller, L., Christensen, L., and Duffy, M.J. (1997). The urokinase-type plasminogen activator system in cancer metastasis: a review. Int. J. Cancer *72*, 1–22.
8. Lijnen, H.R., Silence, J., Lemmens, G., Frederix, L., and Collen, D. (1998). Regulation of gelatinase activity in mice with targeted inactivation of components of the plasminogen/plasmin system. Thromb. Haemost. *79*, 1171–1176.
9. Folkman, J., and Shing, Y. (1992). Angiogenesis. J. Biol. Chem. *267*, 10931–10934.
10. Duffy, M.J., Maguire, T.M., McDermott, E.W., and O'Higgins, N. (1999). Urokinase plasminogen activator: a prognostic marker in multiple types of cancer. J. Surg. Oncol. *71*, 130–135.
11. Look, M.P., and Foekens, J.A. (1999). Clinical relevance of the urokinase plasminogen activator system in breast cancer. APMIS *107*, 150–159.
12. Casella, R., Shariat, S.F., Monoski, M.A., and Lerner, S.P. (2002). Urinary levels of urokinase-type plasminogen activator and its receptor in the detection of bladder carcinoma. Cancer *95*, 2494–2499.
13. Ferno, M., Bendahl, P.O., Borg, A., Brundell, J., Hirschberg, L., Olsson, H., and Killander, D. (1996). Urokinase plasminogen activator, a strong independent prognostic factor in breast cancer, analysed in steroid receptor cytosols with a luminometric immunoassay. Eur. J. Cancer *32A*, 793–801.
14. Pedersen, A.N., Mouridsen, H.T., Tenney, D.Y., and Brunner, N. (2003). Immunoassays of urokinase (uPA) and its type-1 inhibitor (PAI-1) in detergent extracts of breast cancer tissue. Eur. J. Cancer *39*, 899–908.
15. Seetoo, D.Q., Crowe, P.J., Russell, P.J., and Yang, J.L. (2003). Quantitative expression of protein markers of plasminogen activation system in prognosis of colorectal cancer. J. Surg. Oncol. *82*, 184–193.
16. Bogdanov, A., Jr., Wright, S.C., Marecos, E.M., Bogdanova, A., Martin, C., Petherick, P., and Weissleder, R. (1997). A long-circulating co-polymer in "passive targeting" to solid tumors. J. Drug Target. *4*, 321–330.
17. Tung, C.H., Mahmood, U., Bredow, S., and Weissleder, R. (2000). In vivo imaging of proteolytic enzyme activity using a novel molecular reporter. Cancer Res. *60*, 4953–4958.
18. Ntziachristos, V., Tung, C.H., Bremer, C., and Weissleder, R. (2002). Fluorescence molecular tomography resolves protease activity in vivo. Nat. Med. *8*, 757–760.
19. Ke, S.H., Coombs, G.S., Tachias, K., Corey, D.R., and Madison, E.L. (1997). Optimal subsite occupancy and design of a selective inhibitor of urokinase. J. Biol. Chem. *272*, 20456–20462.
20. Klinghofer, V., Stewart, K., McGonigal, T., Smith, R., Sarthy, A., Nienaber, V., Butler, C., Dorwin, S., Richardson, P., Weitzberg, M., et al. (2001). Species specificity of amidine-based urokinase inhibitors. Biochemistry *40*, 9125–9131.
21. Tung, C.H., Bredow, S., Mahmood, U., and Weissleder, R. (1999). Preparation of a cathepsin D sensitive near-infrared fluorescence probe for imaging. Bioconjug. Chem. *10*, 892–896.
22. Gruber, H.J., Hahn, C.D., Kada, G., Riener, C.K., Harms, G.S., Ahrer, W., Dax, T.G., and Knaus, H.G. (2000). Anomalous fluorescence enhancement of Cy3 and cy3.5 versus anomalous fluorescence loss of Cy5 and Cy7 upon covalent linking to IgG and noncovalent binding to avidin. Bioconjug. Chem. *11*, 696–704.
23. Mishra, A., Behera, R.K., Behera, P.K., Mishra, B.K., and Behera, G.B. (2000). Cyanines during the 1990s: A Review. Chem. Rev. *100*, 1973–2012.
24. Mahmood, U., Tung, C.H., Bogdanov, A., Jr., and Weissleder, R. (1999). Near-infrared optical imaging of protease activity for tumor detection. Radiology *213*, 866–870.
25. Carmeliet, P., Schoonjans, L., Kieckens, L., Ream, B., Degen, J., Bronson, R., De Vos, R., van den Oord, J.J., Collen, D., and Mulligan, R.C. (1994). Physiological consequences of loss of plasminogen activator gene function in mice. Nature *368*, 419–424.
26. Netzel-Arnett, S., Mitola, D.J., Yamada, S.S., Chrysovergis, K., Holmbeck, K., Birkedal-Hansen, H., and Bugge, T.H. (2002). Collagen dissolution by keratinocytes requires cell surface plasminogen activation and matrix metalloproteinase activity. J. Biol. Chem. *277*, 45154–45161.
27. Gutierrez, L.S., Schulman, A., Brito-Robinson, T., Noria, F., Ploplis, V.A., and Castellino, F.J. (2000). Tumor development is retarded in mice lacking the gene for urokinase-type plasminogen activator or its inhibitor, plasminogen activator inhibitor-1. Cancer Res. *60*, 5839–5847.
28. Sawaya, R., and Highsmith, R. (1988). Plasminogen activator activity and molecular weight patterns in human brain tumors. J. Neurosurg. *68*, 73–79.
29. Weissleder, R., Tung, C.H., Mahmood, U., and Bogdanov, A., Jr. (1999). In vivo imaging of tumors with protease-activated near-infrared fluorescent probes. Nat. Biotechnol. *17*, 375–378.
30. Bremer, C., Tung, C.H., and Weissleder, R. (2001). In vivo molecular target assessment of matrix metalloproteinase inhibition. Nat. Med. *7*, 743–748.
31. Rudolph, M.J., Illig, C.R., Subasinghe, N.L., Wilson, K.J., Hoffman, J.B., Randle, T., Green, D., Molloy, C.J., Soll, R.M., Lewandowski, F., et al. (2002). Design and synthesis of 4,5-disubstituted-thiophene-2-amidines as potent urokinase inhibitors. Bioorg. Med. Chem. Lett. *12*, 491–495.